Role of the Regulatory Gene *rirA* in the Transcriptional Response of *Sinorhizobium meliloti* to Iron Limitation†

Tzu-Chiao Chao, Jens Buhrmester, Nicole Hansmeier, Alfred Pühler,
and Stefan Weidner*

*Lehrstuhl für Genetik, Fakultät für Biologie, Universität Bielefeld,
Postfach 100131, D-33501 Bielefeld, Germany*

A regulatory network of *Sinorhizobium meliloti* genes involved in adaptation to iron-limiting conditions and the involvement of the rhizobial iron regulator gene (*rirA*) were analyzed by mutation and microarray analyses. A constructed *S. meliloti rirA* mutant exhibited growth defects and enhanced H_2O_2 sensitivity in the presence of iron, but symbiotic nitrogen fixation was not affected. To identify iron-responsive and RirA-regulated *S. meliloti* genes, a transcriptome approach using whole-genome microarrays was used. Altogether, 45 genes were found to be jointly derepressed by mutation of *rirA* and under different iron-limited conditions. As expected, a number of genes involved in iron transport (e.g., *hmuPSTU*, *shmR*, *rhbABCDEF*, *rhtX*, and *rhtA*) and also genes with predicted functions in energy metabolism (e.g., *fixN3*, *fixP3*, and *qxtAB*) and exopolysaccharide production (e.g., *exoY* and *exoN*) were found in this group of genes. In addition, the iron deficiency response of *S. meliloti* also involved *rirA*-independent expression changes, including repression of the *S. meliloti* flagellar regulon. Finally, the RirA modulon also includes genes that are not iron responsive, including a gene cluster putatively involved in Fe-S cluster formation (*sufA*, *sufS*, *sufD*, *sufC*, and *sufB*).

Iron is an essential micronutrient for almost all known organisms. Due to the ready interconversion between the reduced Fe^{2+} ferrous form and the oxidized Fe^{3+} ferric form, iron is a versatile component for incorporation as a biocatalyst or electron carrier into proteins that are involved in a number of essential metabolic and enzymatic functions. In particular, rhizobia, a diverse group of symbiotic soil bacteria belonging to the genera *Rhizobium*, *Bradyrhizobium*, *Mesorhizobium*, *Azorhizobium*, and *Sinorhizobium*, have a special demand for iron. These so-called root nodule bacteria are known for their ability to establish nitrogen-fixing symbioses with their legume hosts. During this symbiotic interaction root nodules are formed, in which the bacteria fix atmospheric nitrogen after differentiation into bacteroids (61). Many enzymes necessary for the reduction of atmospheric nitrogen (e.g., nitrogenase and nitrogenase reductase) contain iron compounds as cofactors. In addition, the bacteroids have a very high respiratory demand, requiring an abundance of cytochromes and other ferro-proteins (14). Thus, rhizobia not only need to compete successfully with other soil organisms for iron in order to propagate in the free-living state but also need to satisfy their high iron demand during symbiosis.

Although iron is abundant in the Earth's soil, under physiological conditions it is mainly present as insoluble ferric iron. Accordingly, bacteria have evolved a number of transport systems in order to ensure a sufficient supply of iron. A common mechanism employed by most bacteria is the synthesis and secretion of siderophores, which are low-molecular-weight ligands that specifically bind ferric iron with high affinity. The ferri-siderophore complexes are then transported into the cell via cognate transporters. A number of siderophores have been characterized in different rhizobia; these include the trihydroxamate vicibactin of *Rhizobium leguminosarum* (10, 11), the amino polycarboxylic acid siderophore of *Sinorhizobium meliloti* DM4 (59), and the citrate-based dihydroxamate rhizobactin 1021 produced by *S. meliloti* 1021 (46). In addition to their own or exogenous ferri-siderophores, rhizobia are also known to use a wide range of other iron sources, including ferric citrate, heme, and hemoglobin (3, 11, 39, 71). This flexibility with regard to iron utilization probably reflects adaptation to complex environmental conditions and underlines the importance of iron acquisition for rhizobia.

Despite the importance of iron, high concentrations of this metal can lead to generation of hydroxyl radicals as a result of the Fenton chemistry. Therefore, iron uptake is usually strictly regulated. In many gram-negative bacteria and some gram-positive bacteria the ferric uptake regulator (Fur) has been established as a central regulator of iron-responsive genes (1, 17, 22, 23). In the sequenced genome of *S. meliloti* 1021, the microsymbiont of alfalfa, a Fur homologue is encoded (9, 19), but recently we demonstrated that this protein is primarily involved in the regulation of the Mn^{2+} transporter operon *sitABCD* (12), a finding that was verified independently by Platero et al. (47). A similar role of Fur was also found in *R. leguminosarum* (15, 70). It is therefore obvious that in *S. meliloti* and *R. leguminosarum* iron-dependent regulation is implemented very differently than it is in other gram-negative bacteria. In *R. leguminosarum*, Todd and colleagues have identified a regulator termed RirA (rhizobial iron regulator) which has been shown to be involved in the regulation of several iron-responsive genes (64). Additionally, proteome analyses indicated that over 100 proteins were differentially expressed

* Corresponding author. Mailing address: Lehrstuhl für Genetik, Fakultät für Biologie, Universität Bielefeld, Postfach 100131, D-33501 Bielefeld, Germany. Phone: 49 521 106-2034. Fax: 49 521 106-5626. E-mail: Stefan.Weidner@CeBiTec.Uni-Bielefeld.de.

TABLE 1. Bacterial strains and plasmids

Strain or plasmid	Characteristics	Reference
Sinorhizobium meliloti strains		
Rm1021	Spontaneous mutant of wild-type strain RU47, Sm^r	35
Rm1021-TR2	Rm1021 derivative, Δ*rirA*	This study
Rm1021-TR2-3	Rm1021 derivative, Δ*rirA* Δ*rhrA*	This study
Escherichia coli strains		
DH5αMCR	F$^-$ *endA1 supE44 thi-1* λ$^-$ *recA1 gyrA96 relA1 deoR* Δ(*lacZYA-argF*)*U169* φ80d*lacZ*ΔM15 *mcrA* Δ(*mrr hsdRMS mcrBC*)	20
S17-1	*E. coli* 294::[RP4-2(Tc::Mu)(Km::Tn7)] *pro res* Δ*recA* Tp^r	57
Plasmid		
pK18mobsacB	pUC18 derivative, *sacB lacZ*α Km^r, mobilizable	53

in an *R. leguminosarum rirA* mutant, and 10 of these proteins were identified by mass spectrometry (65).

The *R. leguminosarum* RirA protein does not exhibit significant sequence homology to known iron-responsive regulators, such as Fur, DtxR (7), or Irr (21), and belongs to the Rrf2 family of putative transcription regulators. Other members of this protein family include NsrR, which is involved in regulating a nitrite reductase in *Nitrosomonas europaea* (4), Rrf2, a regulator of cytochrome synthesis in *Desulfovibrio vulgaris* (30), and IscR, an iron-sulfur protein involved in the regulation of Fe-S cluster formation (54). Hence, the members of this family of regulators appear to have very diverse functions in different eubacterial species.

There is an *rirA* homologue in *S. meliloti* (64), but its role in this symbiont is still unknown. In this study we analyzed the relevance of the *S. meliloti rirA* gene for controlling iron homeostasis during free-living growth and symbiosis. As the *S. meliloti rirA* gene is a likely candidate for a global iron-dependent regulator, whole-genome microarrays were utilized to identify the extent of RirA-regulated genes. These experiments were complemented with transcriptome profiling of changes in global iron-dependent expression in order to identify the mechanism with which *S. meliloti* adapts to iron-limiting conditions and to define the relevance of *rirA* for coordinating the iron deficiency response.

MATERIALS AND METHODS

Bacterial strains, plasmids, and media. The bacterial strains and plasmids used in this study are shown in Table 1. Strains of *Escherichia coli* were routinely cultured at 37°C in antibiotic medium no. 3 (Oxoid, Wesel, Germany). *S. meliloti* strains were cultivated at 30°C either in tryptone yeast (TY) complex medium (6) or in Vincent minimal medium (VMM) (67). VMM was prepared without iron. A final FeCl$_3$ concentration of 37 μM was used for iron-sufficient growth in VMM, and an FeCl$_3$ concentration of 0.37 μM was used for iron-deficient growth in VMM. Other iron sources and the concentrations used are indicated below. Iron-limited TY medium was prepared by adding the iron chelator 2,2′-dipyridyl to a final concentration 200 μM. When appropriate, antibiotics were added at the following concentrations: neomycin, 100 μg ml^{-1}; kanamycin, 50 μg ml^{-1}; and streptomycin, 600 μg ml^{-1}. Glassware was washed with 50 mM EDTA and 6 M HCl before it was thoroughly rinsed with water.

DNA manipulations. The protocols of Sambrook et al. (52) were used for routine manipulations of plasmid and chromosomal DNA. Mutated DNA fragments containing either a 342-bp deletion in the *rirA* gene or a 810-bp deletion in the *rhrA* gene were constructed by gene SOEing (27). In a first PCR regions up- and downstream of the desired deletion were amplified, and then they were fused in a second PCR. The deletion constructs obtained were subsequently cloned into the suicide vector pK18mobsacB, which allows sucrose selection for vector loss (53). The resulting plasmids were conjugated into *S. meliloti* via *E. coli* S17-1 to introduce deletions by allelic exchange. Mutants were verified by PCR and Southern hybridization.

CAS siderophore assay. Chrome azurol S (CAS) assay mixtures for siderophore detection were prepared as described by Schwyn and Neilands (55). Supernatants of *S. meliloti* cultures grown in VMM containing various concentrations of FeCl$_3$ were mixed 1:1 with a CAS assay solution. After equilibrium was reached, the absorbance at 630 nm was measured. The relative siderophore activity was determined by measuring optical density ratios of different cultures.

H$_2$O$_2$ challenge. To test for H$_2$O$_2$ sensitivity, overnight cultures of *S. meliloti* wild-type strain Rm1021 and *rirA* mutant Rm1021-TR2 were washed, and equal amounts of the two strains were incubated for 4 h in iron-free VMM and VMM containing 60 μM FeCl$_3$, respectively. After this, the samples were exposed to 50 mM H$_2$O$_2$ for 2 h. The survival rate was determined by comparing the number of CFU for H$_2$O$_2$-treated samples to the number of CFU for untreated control samples after incubation for 2 days on TY agar plates at 30°C.

Assays to determine nitrogen fixation efficiency in the *S. meliloti-Medicago sativa* symbiosis. Nodulation tests were performed as described by Rolfe et al. (50). Solutions a to c for the plant agar plates (solution a contained 294 g/liter CaCl$_2$ · 2H$_2$O; solution b contained 50 g/liter KH$_2$PO$_4$; solution c contained 123 g/liter MgSO$_4$, 87 g/liter K$_2$SO$_4$, 0.247 g/liter H$_3$BO$_3$, 0.288 g/liter ZnSO$_4$, 0.1 g/liter CuSO$_4$ · 5H$_2$O, 0.056 g/liter CoSO$_4$ · 7H$_2$O, and 0.048 g/liter NaMo$_4$ · 2H$_2$O) were autoclaved separately. Then 0.5 ml of each solution was added to 1 liter autoclaved water containing 15 g agar. FeSO$_4$ was added as an iron source at final concentrations of 5, 10, and 15 μM to the medium. Alfalfa (*M. sativa* L. cv. europe) seeds were sterilized with 32% HCl for 30 min and then washed with sterile water. After germination, seedlings were placed on nodulation plates and inoculated with equal amounts (6 × 10^7 CFU) of washed wild-type and mutant cells. Plants were weighed after 30 days of growth, and the nitrogen fixation activity was tested by the acetylene reduction assay (50).

S. meliloti transcript profiling using the genome-wide SM6kOligo microarray. For identification of the RirA modulon, *S. meliloti* wild-type strain Rm1021 and *rirA* mutant Rm1021-TR2 were cultivated in VMM containing 37 μM FeCl$_3$. For transcriptome profiling of iron-regulated genes, the *S. meliloti* wild-type Rm1021 strain was grown in either TY medium (iron-sufficient complex medium), TY medium containing 200 μM 2,2′-dipyridyl (iron-limited complex medium), VMM containing 37 μM FeCl$_3$ (iron-sufficient minimal medium), or VMM containing 0.37 μM FeCl$_3$ (iron-limited minimal medium). All cultures were incubated in 250-ml Erlenmeyer flasks with shaking at 150 rpm at 30°C until the optical density at 580 nm was 0.9 before they were harvested. Cells were centrifuged (10,000 × *g*, 1 min, 4°C) and then immediately frozen in liquid nitrogen. For total-RNA isolation an RNeasy mini kit (QIAGEN, Hildesheim, Germany) was used. Cells were disrupted in the RLT buffer provided in the kit in Fast Protein tubes (Qbiogene, Carlsbad, CA) using a Ribolyser (30 s; speed, 6.5; Hybaid, Heidelberg, Germany) before RNA isolation using the RNeasy mini kit RNA purification protocol. Fluorescent labeling of cDNA by amino-allyl dye coupling was performed as described by de Risi (http://www.microarrays.org/protocols.html). For this study the Sm6kOligo microarrays described by Krol and Becker (32) were used. Hybridization and image acquisition of the microarrays were performed as described previously (5, 51). For acquisition of the mean signal and mean local background intensity for each spot of the microarray, the ImaGene 5.0 software (Biodiscovery Inc., Los Angeles, CA) for spot detection, image segmentation, and signal quantification was used. The log$_2$ value of the intensity ratios (M_i) was calculated for each spot as follows: $M_i = \log_2(R_i/G_i)$, where $R_i = I_{\mathrm{ch1}i} - \mathrm{Bg}_{\mathrm{ch1}i}$ and $G_i = I_{\mathrm{ch2}i} - \mathrm{Bg}_{\mathrm{ch2}i}$ ($I_{\mathrm{ch1}i}$ and $I_{\mathrm{ch2}i}$ are the intensities of spots in channels 1 and 2, respectively, and $\mathrm{Bg}_{\mathrm{ch1}i}$ and $\mathrm{Bg}_{\mathrm{ch2}i}$ are the background intensities of spots in channels 1 and 2, respectively). The mean intensity (A_i) was calculated for each spot as follows: $A_i = \log_2(R_iG_i)^{0.5}$. A normalization method based on local regression that accounts for intensity spatial dependence

in dye biases was used (73). Normalization and t-statistics were carried out using the Emma 1.1 microarray data analysis software (16). The expression of a gene was considered significantly different if the P value was ≤ 0.05, the $\log_2$ ratio of the intensities (M value) was ≥ 1 or ≤ -1, and the mean intensity (A value) was ≥ 7. The microarray results were verified for specific genes (*rhbA*, *shmR*, and *hmuS*) by quantitative reverse transcription-PCR using a QuantiTect SYBR Green reverse transcription-PCR kit (QIAGEN, Hildesheim, Germany) according to the manufacturer's instructions. The measurements were obtained with a LightCycler instrument (Roche, Mannheim, Germany). The *rhbA* and *shmR* genes were chosen since previous reports showed that there was iron-responsive regulation of these genes (3, 34). Iron-dependent regulation of the *hmuS* genes was confirmed by glucuronidase assays (data not shown).

RESULTS AND DISCUSSION

Mutational analysis of the *S. meliloti* *rirA* gene suggested that it is involved in the regulation of iron metabolism. One of the objectives of this work was to elucidate iron-dependent regulation in *S. meliloti*. As we demonstrated previously that the *S. meliloti* *fur* gene is not involved in iron-dependent regulation, we focused on the rhizobial iron regulator gene *rirA*. The *rirA* gene was initially identified in *R. leguminosarum* as a possible regulator of iron-responsive genes (64). In *S. meliloti* a gene (SMc00785) homologous to the *R. leguminosarum* *rirA* gene was identified, which has been annotated to encode a hypothetical protein. The deduced protein had a predicted molecular mass of 17 kDa and exhibited very high levels of homology to the RirA repressor of *R. leguminosarum* (84% identity, 93% positive). Consequently, we renamed the corresponding *S. meliloti* open reading frame (SMc00785) *rirA*. Other close homologues of the *S. meliloti* RirA protein occur in the closely related plant pathogen *Agrobacterium tumefaciens*, *Mesorhizobium loti*, and different *Brucella* and *Bartonella* species. In none of these proteins could a significant helix-turn-helix motif, which is typical of many bacterial transcriptional regulators, be identified by bioinformatic approaches. The *S. meliloti* *rirA* gene is flanked downstream by genes encoding a putative dipeptide transporter (*dppA1-F1*) and upstream by a gene coding a putative periplasmic iron binding protein (SMc00784).

In order to assess the role of the *S. meliloti* *rirA* gene in regulation of global iron metabolism, a marker-free *S. meliloti* *rirA* deletion mutant designated Rm1021-TR2 (Table 1) was constructed and used for further studies. As we hypothesized that the *rirA* gene might be the central regulator of iron metabolism, we tested the influence of iron status on the growth of the *rirA* mutant. To do this, *S. meliloti* wild-type strain Rm1021 and *rirA* mutant Rm1021-TR2 were grown in VMM containing different iron sources. In medium containing 37 μM FeCl$_3$ as the sole iron source, the *rirA* mutant exhibited a reduced growth rate (Fig. 1a). This phenotype was partially recovered in minimal medium containing only 0.37 μM FeCl$_3$ (Fig. 1b). This reduction in growth of the *rirA* mutant was apparently connected to iron availability and may have been caused by oxidative stress due to derepressed iron uptake. With hemin as the iron source, virtually no growth of the *rirA* mutant was observed (Fig. 1c). Supplementation with other iron sources did not restore growth if hemin was present (data not shown), indicating that deregulated accumulation of this potentially toxic compound (63), rather than the inability of the *rirA* mutant strain to utilize hemin as an iron source, was responsible for the growth defects.
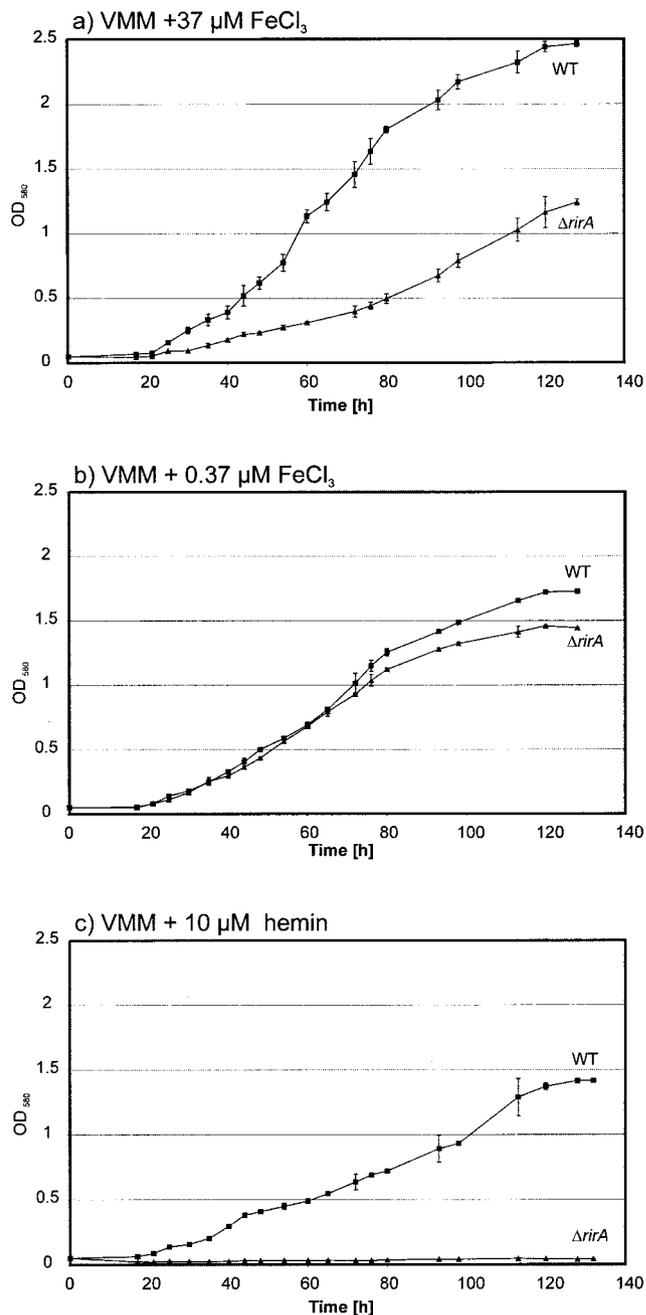

FIG. 1. Effects of the *rirA* mutation on growth rates of *S. meliloti* strains. Overnight cultures of *S. meliloti* wild-type strain Rm1021 (WT) and *rirA* mutant Rm1021-TR2 (ΔrirA) were washed and diluted in fresh minimal medium containing 37 μM FeCl$_3$ (a), 0.37 μM FeCl$_3$ (b), or 10 μM hemin (c) as the sole iron source. Samples were taken, and their optical densities at 580 nm (OD$_{580}$) were determined. The error bars indicate the standard deviations calculated from six independent cultures.

Further evidence for the involvement of the *rirA* gene in regulating iron acquisition was obtained by semiquantitative liquid CAS assays in which the siderophore concentrations in supernatants of the *rirA* mutant were compared to those in wild-type cultures. When cultivated under low-iron conditions (no FeCl$_3$), both strains exhibited siderophore production, but the amount in the *rirA* mutant was ~125-fold higher. Addition

of 37 μM FeCl₃ to the culture medium abolished siderophore production in the wild type but did not affect siderophore accumulation in the *rirA* mutant (data not shown). Thus, the sensitivity of the *rirA* mutant to high iron concentrations might be at least partially caused by derepression of siderophore-dependent iron uptake mechanisms.

Since oxidative stress caused by the Fenton reaction in the presence of iron can be enhanced by low doses of H_2O_2, we tested the effect of the *rirA* mutation on H_2O_2 sensitivity in the presence of FeCl₃ to ascertain whether the growth deficits of the *rirA* mutant were a result of enhanced oxidative stress. When preincubated in medium containing no added iron sources before challenge with H_2O_2, the *rirA* mutant showed only a slightly lower survival ratio (46% ± 3%) than the wild type (58% ± 4%). However, the survival ratio of *rirA* mutant cells which were preincubated in iron-containing medium was reduced to only 4% ± 0.5%, whereas the viability of the wild type remained largely unchanged (40% ± 2%).

In conclusion, the bioassays indicated that a mutation in *rirA* leads to harmful accumulation of FeCl₃ or hemin, resulting in reduced viability due to oxidative stress. In other gram-negative bacteria, like *E. coli* (66), *Yersinia pestis* (62), and *Pseudomonas aeruginosa* (24), a *fur* mutation led to iron overload, resulting in iron-dependent growth phenotypes similar to those exhibited by the *S. meliloti rirA* mutant. Our data therefore suggested that the importance of the *S. meliloti rirA* gene for maintaining the intracellular iron balance below toxic levels is similar to the importance of *fur* in other bacteria. It is interesting that in *R. leguminosarum* an *rirA* mutation resulted in an iron-independent growth phenotype (64), indicating that there may be a different mode of *rirA*-mediated regulation and oxidative stress avoidance in *R. leguminosarum*.

Since deregulation of iron uptake caused by the *rirA* mutation had strong effects on the viability of *S. meliloti*, we speculated that the symbiotic properties might also be affected. To test this, *M. sativa* seedlings were inoculated with either the wild-type strain or the *rirA* mutant on plant medium containing FeSO₄ at concentrations between 5 and 15 μM. However, no significant differences in nodulation efficiency, foliage fresh weight, or nitrogen fixation rate between plants inoculated with the wild type and plants inoculated with the mutant were found (data not shown). In conclusion, our results indicated that *rirA* is essential for maintaining a balanced iron content in the cell during iron-sufficient free-living growth, but not during symbiosis. It is therefore possible that in planta iron uptake is regulated independent of *rirA*; alternatively, in nodules the iron availability might be limited, or iron could be provided in a form that does not require strict regulation by *rirA*.

Transcriptional profiling of the *S. meliloti rirA* mutant and the wild-type strain supported the hypothesis that the *rirA* gene has a regulatory function in iron metabolism. In order to define the RirA modulon, transcriptome studies utilizing Sm6kOligo microarrays (32) were performed. The complete set of genes affected by the *rirA* mutation was identified by comparing the transcriptomes of the *rirA* mutant Rm1021-TR2 and the wild-type strain Rm1021 cultivated in iron-sufficient VMM. Duplicate samples were taken from three independent cultures of each strain, which yielded a total of six replicates for each experimental microarray set. RNA isolation, labeling, hybridization, and data analysis were performed as described

in Materials and Methods. Only genes with statistically significant ($P \leq 0.05$) changes in expression of twofold or more were considered. Using this approach, the expression of 195 genes was found to be significantly changed by the *rirA* mutation. Of these 195 genes, 132 were induced, whereas only 63 genes were repressed in the *rirA* mutant compared to the wild type. Figure 2a shows the results of microarray experiments expressed by plotting the $\log_2$ expression ratio (*M* value) versus the mean signal intensity (*A* value) for each gene. As expected, many of the most highly induced genes (induction levels, 8- to 181-fold) belonged to the previously characterized rhizobactin 1021 synthesis and uptake cluster (including *rhbABCDEF* and *rhtX*) (34), further confirming the role of *rirA* as a repressor of iron uptake genes. In contrast, the only highly repressed gene that was found was the *rirA* gene itself, whose expression was reduced fourfold or more, an obvious result of deletion of this gene.

Transcriptome profiling of the *S. meliloti* wild-type strain grown with high and low iron concentrations defined the iron deficiency stimulon. Assuming that RirA is a global regulator of iron-responsive genes, a large overlap between genes affected in expression by the *rirA* mutation and genes affected in expression by iron limitation was expected. Accordingly, two sets of microarray experiments were performed under iron-limited conditions to assess the role of *rirA* in coordinating gene expression in response to iron availability and also to identify other *rirA*-independent iron-regulated genes. Two different types of media were used for these experiments, defined VMM and complex TY medium, both either iron deficient or iron sufficient, in order to distinguish between iron-specific and medium-specific expression changes. The optimal culture conditions under which an iron deficiency response was elicited but which still allowed consistent growth were ascertained by monitoring the viability of *S. meliloti* cells incubated either in TY medium with increasing concentrations of the iron chelator 2,2′-dipyridyl or in VMM with various concentrations of FeCl₃ as the sole iron source. At the same time the siderophore production was measured by using a semiquantitative CAS assay as a marker for an iron deficiency response (data not shown). Consequently, we decided to compare the transcriptome of *S. meliloti* wild-type cells grown in VMM containing 0.37 μM FeCl₃ (iron-limited VMM) to the transcriptome of cells cultivated in VMM containing 37 μM FeCl₃ (iron-sufficient VMM); likewise, the gene expression of cultures grown in TY medium containing the iron chelator 2,2′-dipyridyl at a concentration of 200 μM (iron-limited TY medium) was compared to the gene expression of cells grown in TY medium without additives.

In iron-limited VMM the expression patterns of 378 genes were altered compared to the patterns observed for growth in iron-sufficient VMM. A total of 199 of these genes were induced by iron limitation, and 179 were repressed. An overview of genes with the greatest increases in mRNA abundance in iron-limited VMM, as shown in a scatter plot (Fig. 2b), revealed a significant consensus for the most highly induced genes in the *S. meliloti rirA* mutant (Fig. 2a). In contrast, the most highly repressed genes during growth in iron-limited VMM were involved in chemotaxis and cell motility, which was not apparent in the *rirA* mutant.

Finally, with 2,2′-dipyridyl-induced iron limitation in TY medium 318 genes were found to be differentially expressed

FIG. 2. Scatter plots of the microarray-based analysis of *S. meliloti* gene expression affected by iron limitation and the *rirA* mutation. The plots show the logarithmic mean signal ratio (M-value) versus the logarithmic mean signal intensity (A-value) obtained by comparison of the transcriptomes of *S. meliloti rirA* mutant Rm1021-TR2 (ΔrirA) and *S. meliloti* wild-type strain Rm1021 (WT) (a), *S. meliloti* wild-type cells grown in iron-limited VMM and cells grown in iron-sufficient VMM (b), and *S. meliloti* wild-type cells incubated in iron-limited TY medium and cells grown in iron-sufficient TY medium (c). A number of genes with the greatest changes in mRNA abundance are indicated. The functions of the genes indicated are shown in Tables 2 and 3.

(Fig. 2c). Of these 318 genes, 184 were upregulated, and 134 were downregulated. The scatter plots derived from these microarray results demonstrated that there was a high correlation between the most highly induced and repressed genes under both sets of iron-limited conditions, indicating that a comparison of these conditions is suitable for elucidating the transcriptome response of *S. meliloti* for dependence on iron availability.

TABLE 2. *S. meliloti* genes significantly induced under iron-limiting conditions and in the *rirA* mutant[a]

Open reading frame	Gene and/or description	Expression ratio[b]		
		VMM	TY medium	ΔrirA
SMa0002	*fdoG*, probable FdoG formate dehydrogenase-O alpha subunit	−0.42	2.13	1.05
SMa0142	Possible protease	1.60	1.29	1.08
SMa0172	Conserved hypothetical protein	1.27	1.17	0.96
SMa0312	Hypothetical protein	2.43	1.74	2.09
SMa0314	Hypothetical protein	1.24	0.92	1.21
SMa0316	Conserved hypothetical protein	2.31	0.90	1.56
SMa0320	Putative dehydrogenase	1.81	0.49	1.68
SMa0612	*fixN3*, cytochrome *c* oxidase subunit 1	1.97	1.61	1.26
SMa0617	*fixP3*, cytochrome *c* oxidase membrane-anchored subunit	1.27	1.05	1.62
SMa0621	*fixI2*, E1-E2-type cation ATPase	1.00	0.52	1.11
SMa0994	Hypothetical protein	1.37	1.92	1.08
SMa1461	Putative muconate cycloisomerase	1.13	0.66	1.47
SMa1683	Putative arylsulfatase	2.57	1.02	1.74
SMa1686	Putative two-component response regulator	1.05	1.09	0.54
SMa1745	Putative iron ABC transporter permease	1.09	0.51	1.39
SMa1746	Putative iron ABC transporter periplasmic binding protein	1.98	1.96	2.41
SMa1749	Putative transcriptional regulator	0.47	1.16	1.23
SMa1860	Putative ABC transporter periplasmic binding protein	2.13	1.05	1.02
SMa1985	Hypothetical protein	1.09	0.83	1.56
SMa2259	Hypothetical protein	1.25	0.77	1.36
SMa2294	*mrcA2*, probable penicillin binding protein	1.35	1.47	
SMa2337	*rhtX*, rhizobactin 1021 transporter	4.95	3.39	4.96
SMa2339	Putative siderophore biosynthesis protein	5.09	3.17	6.28
SMa2400	*rhbA*, rhizobactin 1021 biosynthesis protein	7.86	5.20	7.50
SMa2402	*rhbB*, rhizobactin 1021 biosynthesis protein	5.81	4.85	5.78
SMa2404	*rhbC*, rhizobactin 1021 biosynthesis protein	4.34	2.02	4.74
SMa2406	*rhbD*, rhizobactin 1021 biosynthesis protein	5.21	3.11	5.40
SMa2408	*rhbE*, rhizobactin 1021 biosynthesis protein	7.19	4.66	6.70
SMa2410	*rhbF*, rhizobactin 1021 biosynthesis protein	6.38	4.47	6.38
SMa2412	*rhrA*, transcriptional activator	1.40	1.75	2.42
SMa2414	*rhtA*, rhizobactin 1021 receptor	4.72	3.96	4.27
SMb20022	Conserved hypothetical protein	1.22	1.23	1.36
SMb20072	Putative rhizopine binding protein	1.06	3.46	0.37
SMb20099	Putative trehalose synthase protein	1.81	1.17	1.18
SMb20127	Hypothetical protein	1.36	0.56	2.88
SMb20203	*cbbR*, probable transcriptional regulator protein	1.07	0.63	1.38
SMb20545	Hypothetical protein	1.19	0.15	1.31
SMb20600	Hypothetical protein	1.73	1.43	0.75
SMb20755	*pccB*, putative propionyl-coenzyme A carboxylase beta chain protein	1.18	2.07	0.24
SMb20757	*bhbA*, methylmalonyl-coenzyme A mutase protein	1.40	2.07	0.52
SMb20924	*abfA*, putative alpha-L-arabinofuranosidase protein	1.76	0.70	1.44
SMb20946	*exoY*, galactosyltransferase protein	2.06	1.43	1.18
SMb20949	*exoV*, putative pyruvyltransferase protein	1.46	0.90	1.04
SMb20959	*exoO*, glucosyltransferase protein	0.70	1.12	1.37
SMb20960	*exoN*, UDP-glucose pyrophosphorylase protein	1.72	1.41	1.41
SMb20993	Putative monooxygenase protein	1.05	0.45	1.09
SMb21285	Conserved hypothetical protein	1.57	1.65	2.05
SMb21337	Putative oxidoreductase	1.43	1.48	0.65
SMb21432	Putative iron ABC transporter periplasmic solute binding protein	1.35	2.18	2.10
SMb21456	Hypothetical protein	1.88	1.33	0.60
SMb21464	Putative transcriptional regulator GntR family protein	1.07	0.10	1.42
SMb21487	*cyoA*, putative cytochrome *o* ubiquinol oxidase chain II protein	−0.51	2.88	2.94
SMb21488	*cyoB*, putative cytochrome *o* ubiquinol oxidase chain I protein	−0.29	2.76	2.55
SMb21489	*cyoC*, putative cytochrome *o* ubiquinol oxidase chain III protein	−0.09	2.64	2.08
SMb21690	*exoW*, glucosyltransferase protein	2.07	1.22	1.13
SMc00062	Hypothetical protein	1.05	0.88	1.63
SMc00086	*cycG*, putative diheme cytochrome *c* type signal peptide protein	1.90	−0.01	1.52
SMc00136	Putative oxidoreductase protein	1.39	1.37	0.60
SMc00235	*trpD*, probable anthranilate phosphoribosyltransferase protein	1.44	−0.06	1.74
SMc00301	Conserved hypothetical protein	0.40	1.02	1.31
SMc00338	Conserved hypothetical protein	1.78	1.23	0.82
SMc00371	Conserved hypothetical protein	1.09	1.11	0.27
SMc00401	Conserved hypothetical protein	1.72	1.70	2.99
SMc00402	Putative iron-regulated protein A	1.44	1.49	2.72
SMc00512	Conserved hypothetical protein	1.07	1.07	0.29
SMc00537	Putative transport protein	1.15	0.23	1.43

TABLE 2—*Continued*

Open reading frame	Gene and/or description	Expression ratio[b]		
		VMM	TY medium	ΔrirA
SMc00591	Hypothetical/unknown signal peptide protein	0.21	2.24	1.77
SMc00592	Hypothetical transmembrane protein	0.76	1.81	1.34
SMc00764	Hypothetical or unknown transmembrane protein	1.23	1.43	0.63
SMc00784	Putative iron ABC transporter periplasmic binding protein	1.42	2.86	2.94
SMc00819	*katA*, catalase	3.17	−0.02	1.16
SMc00830	Hypothetical protein	−0.32	1.20	1.08
SMc00832	*glcD*, probable glycolate oxidase subunit protein	1.14	0.56	1.32
SMc00922	Putative transporter transmembrane protein	1.20	0.55	1.06
SMc01016	Hypothetical protein	1.09	1.75	0.71
SMc01022	Putative cytochrome transmembrane protein	2.16	1.00	1.28
SMc01095	*mexF1*, probable multidrug efflux system transmembrane protein	0.21	1.04	2.81
SMc01169	*ald*, probable alanine dehydrogenase oxidoreductase protein	1.23	1.48	0.56
SMc01266	Conserved hypothetical protein	1.48	1.48	0.98
SMc01267	Conserved hypothetical protein	0.91	1.31	1.13
SMc01471	*senC*, putative cytochrome *c* oxidase assembly factor transmembrane protein	−0.13	1.47	1.29
SMc01489	Hypothetical protein	2.09	1.30	1.04
SMc01512	*hmuT*, putative hemin ABC transporter periplasmic binding protein	1.33	1.32	3.00
SMc01513	*hmuS*, Putative hemin ABC transporter ATPase	2.39	3.04	4.62
SMc01514	Conserved hypothetical protein	2.20	3.56	5.01
SMc01516	Conserved hypothetical protein	1.34	1.77	2.54
SMc01517	Conserved hypothetical protein	0.53	1.18	2.58
SMc01658	Putative transport protein	1.36	0.98	3.11
SMc01659	Putative iron ABC transporter periplasmic binding protein	1.21	1.87	5.51
SMc01718	Hypothetical transmembrane protein	1.64	1.29	0.66
SMc01747	*hmuP*, putative hemin transport protein	2.30	1.52	3.68
SMc01765	Hypothetical transmembrane protein	0.90	1.43	1.04
SMc01788	Hypothetical protein	2.45	1.92	1.21
SMc01814	Probable glutamate synthase small-chain protein	0.15	2.15	1.17
SMc02047	*gcvT*, probable aminomethyltransferase	1.58	2.68	0.24
SMc02075	Conserved hypothetical protein	1.06	1.12	−0.01
SMc02084	*exbD*, putative polymer transport protein	1.21	1.45	1.99
SMc02085	*exbB*, putative polymer transport protein	1.96	2.60	3.57
SMc02156	Conserved hypothetical protein	1.86	1.34	0.96
SMc02179	Conserved hypothetical protein	1.34	1.05	0.44
SMc02254	*qxtB*, putative quinol oxidase subunit II	1.09	2.66	1.08
SMc02255	*qxtA*, putative quinol oxidase subunit I	1.77	4.62	2.37
SMc02266	Conserved hypothetical protein	1.37	1.48	−0.14
SMc02708	Conserved hypothetical protein	1.04	1.05	0.38
SMc02726	*shmR*, hemin binding outer membrane receptor	3.98	2.90	5.98
SMc02727	Hypothetical protein	1.98	0.46	2.23
SMc02887	Hypothetical protein	2.19	0.78	2.17
SMc03149	Hypothetical protein	0.34	1.38	1.58
SMc03787	Hypothetical protein	1.64	3.19	2.70
SMc03971	*mexF2*, putative multidrug efflux system protein	1.19	1.01	1.10
SMc04049	Putative sulfite oxidase protein	1.11	1.03	0.21
SMc04162	Putative transcription regulator protein	1.39	−0.03	1.69
SMc04164	Hypothetical protein	1.40	1.56	0.92
SMc04206	Putative hemolysin type calcium binding protein	4.90	1.93	2.43

[a] Genes were considered differentially expressed when according to t-statistics the *P* value was <0.05 with an induction level of >twofold. Only genes differentially expressed during at least two sets of microarray experiments were considered.
[b] The expression ratios are expressed as log$_2$ values.

Venn mapping identified the *S. meliloti* genes whose expression was affected by iron availability and/or the *rirA* mutation. A complete overview of all genes with significant changes in expression is provided in Table S1 in the supplemental material. Tables 2 and 3 list genes which are differentially expressed under at least two different conditions. For a closer analysis of these data sets, genes that were differentially expressed during growth in iron-limited VMM, in iron-limited TY medium, or in the *rirA* mutant were plotted in a Venn diagram (Fig. 3).

This led to identification of 136 genes (71 induced genes and 65 repressed genes) that were differentially expressed in both iron-limited media compared to growth under iron-sufficient conditions (Fig. 3, subsets A and B). These up- and downregulated genes are likely to be generally involved in the adaptation of *S. meliloti* to low-iron conditions and were considered to represent the *S. meliloti* iron deficiency stimulon. Of the 71 induced genes of the iron deficiency stimulon, 45 were also found to be induced in the *rirA* mutant (Fig. 3, subset B), thus supporting the hypothesis that *rirA* has a role as a major repressor of iron-responsive genes. In contrast, only 4 of the 65 repressed genes belonging to the iron deficiency stimulon were found to be repressed in the *rirA* mutant and under iron-

TABLE 3. *S. meliloti* genes significantly repressed under iron-limiting conditions and in the *rirA* mutant[a]

Open reading frame	Gene and/or description	Expression ratio[b]		
		VMM	TY medium	Δ*rirA*
SMa0249	Conserved hypothetical protein	−1.12	−1.06	−0.07
SMa0252	Conserved hypothetical protein	−2.32	−1.09	−0.40
SMa1289	Hypothetical protein	−1.68	−1.53	−0.10
SMa2032	Putative nonheme chloroperoxidase	−1.70	−1.92	−1.11
SMb20293	Hypothetical protein	−1.47	−1.21	−0.03
SMb20397	Putative oxidoreductase protein	−2.85	−1.69	−0.47
SMb20649	*nadE1*, putative NH₃-dependent NAD⁺ synthetase protein	−1.09	−1.62	−0.02
SMb20650	Putative long-chain fatty acid coenzyme A ligase protein	−1.18	−1.71	−0.02
SMb20651	Hypothetical protein	−2.30	−1.96	0.10
SMb20764	*phnL*, putative phosphonate uptake ABC transporter ATP binding protein	−2.76	−2.31	−0.29
SMb20986	*narB*, putative nitrate reductase large-subunit protein	−1.61	−1.39	0.39
SMb21170	Putative guanylate kinase	−1.08	−1.41	−0.25
SMb21174	*phoT*, phosphate uptake ABC transporter permease protein	−1.07	−1.75	−0.11
SMb21175	*phoE*, phosphate uptake ABC transporter permease protein	−1.70	−1.90	−0.31
SMb21177	*phoC*, phosphate uptake ABC transporter ATP binding protein	−1.36	−1.31	−0.15
SMc00158	Hypothetical protein	−1.41	−2.25	−0.22
SMc00159	Hypothetical protein	−1.70	−2.12	0.12
SMc00283	Putative transcription regulator protein	−3.82	−3.05	−0.64
SMc00335	*rpsA*, 30S ribosomal protein s1	−0.44	−1.14	−1.05
SMc00565	*rplI*, probable 50S ribosomal protein 19	−0.63	−1.12	−1.05
SMc00578	Hypothetical protein	−0.47	−2.05	−1.20
SMc00765	*mcpZ*, probable methyl-accepting chemotaxis protein	−3.68	−3.29	−0.23
SMc00887	Hypothetical protein	−3.35	−3.43	−0.50
SMc00888	Hypothetical protein	−3.08	−3.01	−0.08
SMc00975	*mcpU*, probable chemoreceptor (methyl-accepting chemotaxis) transmembrane protein	−4.11	−4.14	−0.81
SMc00986	Hypothetical protein	−1.83	−1.79	−0.45
SMc00998	Conserved hypothetical signal peptide protein	−1.63	−1.19	0.08
SMc01104	*mcpX*, probable chemoreceptor (methyl-accepting chemotaxis) transmembrane protein	−2.98	−3.67	−0.36
SMc01160	Putative transcriptional regulator protein	−2.51	−0.47	−1.17
SMc01319	*rplJ*, probable 50S ribosomal protein	−1.33	−1.10	−1.51
SMc01326	*tufB*, probable elongation factor Tu protein	−1.04	−0.42	−1.25
SMc01469	*mcpW*, probable methyl-accepting chemotaxis transmembrane protein	−4.38	−3.41	−0.63
SMc01842	Putative methyltransferase transcription regulator protein	−0.49	−2.05	−1.00
SMc01847	Putative methyltransferase protein	−1.40	−1.25	−0.92
SMc02392	Hypothetical protein	−1.39	−1.81	−0.76
SMc02634	Hypothetical transmembrane protein	−2.60	−2.12	−0.91
SMc03004	*mcpE*, putative chemoreceptor (methyl-accepting chemotaxis protein)	−1.36	−1.44	−0.57
SMc03005	Conserved hypothetical protein	−1.21	−1.85	−0.30
SMc03007	*cheA*, chemotaxis protein (sensory transduction histidine kinase)	−2.80	−3.04	−0.57
SMc03008	*cheW1*, chemotaxis protein	−2.04	−2.29	−0.37
SMc03009	*cheR*, chemotaxis protein methyltransferase	−4.21	−3.68	−0.43
SMc03012	*cheD*, chemotaxis protein	−2.18	−2.00	−0.63
SMc03013	Conserved hypothetical protein	−2.07	−2.03	−0.52
SMc03017	Conserved hypothetical protein	−1.61	−1.80	−0.84
SMc03021	*fliM*, flagellar motor switch transmembrane protein	−2.41	−2.83	−0.71
SMc03022	*motA*, chemotaxis (motility protein A)	−2.66	−2.81	−0.80
SMc03023	Conserved hypothetical protein	−2.42	−2.69	−0.76
SMc03024	*flgF*, flagellar basal body rod protein	−3.14	−3.36	−1.00
SMc03027	*flgB*, flagellar basal body rod protein	−3.25	−3.50	−0.84
SMc03028	*flgC*, flagellar basal body rod protein	−1.35	−1.74	−0.59
SMc03029	*fliE*, flagellar hook basal body complex protein	−3.20	−2.72	−0.79
SMc03030	*flgG*, flagellar basal body rod protein	−3.35	−3.30	−0.89
SMc03031	*flgA*, flagellar precursor transmembrane protein	−1.16	−1.88	−0.69
SMc03034	*flgH*, flagellar 1 ring protein precursor	−1.62	−1.97	−0.56
SMc03035	*fliL*, flagellar transmembrane protein	−2.66	−3.11	−1.19
SMc03037	*flaA*, flagellin protein	−3.95	−4.37	−0.11
SMc03038	*flaB*, flagellin protein	−3.97	−3.76	−0.42
SMc03040	*flaC*, flagellin protein	−2.28	−2.36	−0.45
SMc03042	*motB*, chemotaxis protein	−1.84	−2.00	−0.83
SMc03043	*motC*, chemotaxis protein precursor	−1.92	−2.49	−0.96
SMc03044	*motD*, chemotaxis protein	−2.97	−3.04	−0.82
SMc03045	Hypothetical transmembrane protein		−4.50	−1.41
SMc03047	*flgE*, flagellar hook protein	−1.66	−1.61	−0.50
SMc03048	*flgK*, putative flagellar hook-associated protein	−2.50	−1.90	−0.81

Continued on facing page

TABLE 3—*Continued*

Open reading frame	Gene and/or description	Expression ratio[b]		
		VMM	TY medium	Δ*rirA*
SMc03049	*flgL*, putative flagellar hook-associated protein	−3.14	−2.25	−0.85
SMc03051	*flbT*, putative flagellin synthesis repressor protein	−2.21	−1.90	−0.68
SMc03052	*flgD*, putative basal body rod modification protein	−1.94	−1.71	−0.64
SMc03057	Conserved hypothetical transmembrane protein	−1.57	−2.56	−0.74
SMc03071	Hypothetical protein	−1.68	−2.06	−0.56
SMc03072	Conserved hypothetical protein	−3.35	−2.48	−0.62
SMc03242	Probable GTP binding protein	−0.21	−1.10	−1.61
SMc03857	*ffh*, probable signal recognition particle protein	−0.84	−1.16	−1.64
SMc04007	Conserved hypothetical protein	−1.18	−0.86	−1.19
SMc04009	Conserved hypothetical protein	−0.85	−1.03	−1.14
SMc04059	Hypothetical protein	−2.86	−3.23	−0.66
SMc04300	*afuC*, probable iron ABC transporter ATPase	−0.75	−1.40	−1.39
SMc04317	*afuA*, probable iron ABC transporter periplasmic binding protein	−1.52	−1.55	−0.90

[a] Genes were considered differentially expressed when according to t-statistics the P value was <0.05 with a repression level of >two fold. Only genes differentially expressed during at least two sets of microarray experiments were considered.
[b] The expression ratios are expressed as $\log_2$ values.

limiting conditions, further indicating that *rirA* is involved primarily in repression rather than in induction of genes with dependence on iron.

An additional 87 genes of the iron deficiency stimulon (26 upregulated genes and 61 downregulated genes) (Fig. 3, subset A) were not affected by the *rirA* mutation, indicating that other regulatory mechanisms are involved during adaptation of *S. meliloti* to growth under low-iron conditions. Finally, 90 genes were found to be differentially expressed exclusively in the *rirA* mutant, independent of iron availability (Fig. 3, subset C). Several explanations might account for these transcriptome changes: (i) the *rirA* gene might also exert regulatory control on genes in an iron-independent way, (ii) the iron limitation used in this study might not have been sufficient to change the expression above the threshold value that we considered significant, and (iii) the deregulated iron uptake in the *rirA* mutant and the resulting changes in the intracellular iron content might have led to secondary transcriptome changes independent of actual regulation mediated by *rirA*.

S. meliloti genes involved in iron acquisition, energy metabolism, and exopolysaccharide production are induced in the rirA mutant, as well as under iron-limiting conditions. The phenotypic analyses suggested that the *rirA* gene is involved in the repression of iron uptake and siderophore synthesis. In agreement with this, a large number of the 45 genes induced both under iron-limiting conditions and by the *rirA* mutation (Fig. 3, subset B) could be connected to iron acquisition (Table 2). Some of the most highly induced genes were the complete *rhbABCDEF* rhizobactin 1021 synthesis operon (34) and genes encoding the cognate outer membrane receptor (*rhtA*) and the recently characterized inner membrane transporter (*rhtX*) (13) (Fig. 4a). The transcriptional activator *rhrA*, which was demonstrated to be involved in the induction of siderophore synthesis and uptake genes (34), is located in the same gene cluster. Since *rhrA* was induced by iron limitation as well as the *rirA* mutation, indirect regulation of the rhizobactin 1021 synthesis and uptake cluster mediated by *rirA* via *rhrA* appeared to be likely. In fact, in a constructed *rhrA*/*rirA* double mutant
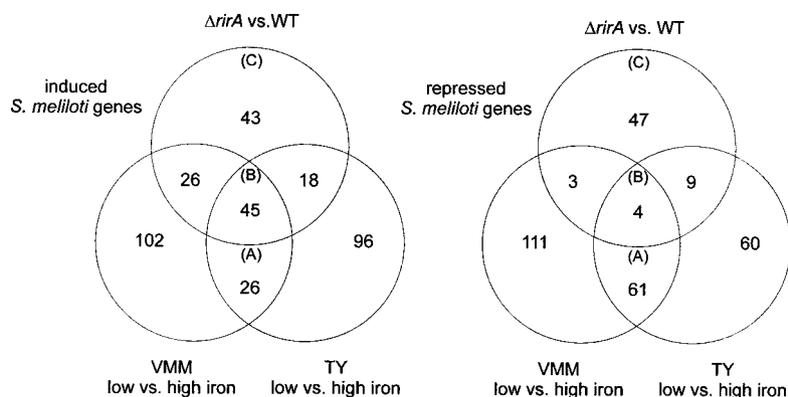

FIG. 3. Venn mapping of *S. meliloti* genes with significantly altered expression obtained from three microarray experiments. The amounts of significantly induced genes (left) and repressed genes (right) were derived from the microarray-based global profiling of iron-responsive and RirA-regulated gene expression in *S. meliloti*. Of special interest were genes that were substantially up- or downregulated under both low- and high-iron conditions but not in the *rirA* mutant (subset A), during all three microarray experiments (subset B), and only in the *rirA* mutant compared to the wild type (WT) (subset C). The Venn diagrams are based on the microarray results shown in Table S1 in the supplemental material.
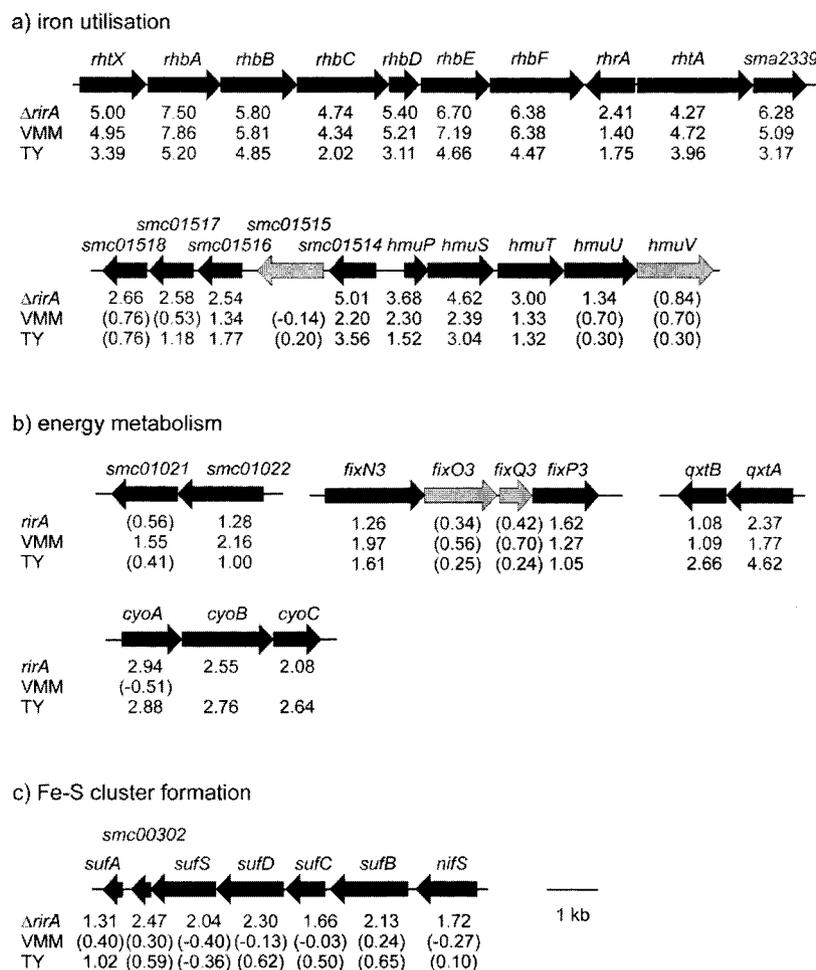
a) iron utilisation

	rhtX	rhbA	rhbB	rhbC	rhbD	rhbE	rhbF	rhrA	rhtA	sma2339
ΔrirA	5.00	7.50	5.80	4.74	5.40	6.70	6.38	2.41	4.27	6.28
VMM	4.95	7.86	5.81	4.34	5.21	7.19	6.38	1.40	4.72	5.09
TY	3.39	5.20	4.85	2.02	3.11	4.66	4.47	1.75	3.96	3.17

	smc01518	smc01517 smc01516	smc01515 smc01514	hmuP	hmuS	hmuT	hmuU	hmuV
ΔrirA	2.66	2.58	2.54	5.01	3.68	4.62	3.00	1.34	(0.84)
VMM	(0.76)	(0.53) 1.34	(-0.14) 2.20	2.30	2.39	1.33	(0.70)	(0.70)
TY	(0.76)	1.18 1.77	(0.20) 3.56	1.52	3.04	1.32	(0.30)	(0.30)

b) energy metabolism

	smc01021	smc01022	fixN3	fixO3	fixQ3	fixP3	qxtB	qxtA
rirA	(0.56)	1.28	1.26	(0.34)	(0.42)	1.62	1.08	2.37
VMM	1.55	2.16	1.97	(0.56)	(0.70)	1.27	1.09	1.77
TY	(0.41)	1.00	1.61	(0.25)	(0.24)	1.05	2.66	4.62

	cyoA	cyoB	cyoC
rirA	2.94	2.55	2.08
VMM	(-0.51)		
TY	2.88	2.76	2.64

c) Fe-S cluster formation

	sufA	sufS	sufD	sufC	sufB	nifS
ΔrirA	1.31 2.47	2.04	2.30	1.66	2.13	1.72
VMM	(0.40)(0.30)	(-0.40)	(-0.13)	(-0.03)	(0.24)	(-0.27)
TY	1.02 (0.59)	(-0.36)	(0.62)	(0.50)	(0.65)	(0.10)

1 kb

FIG. 4. Clustered *S. meliloti* genes whose expression is affected by iron availability and by the *rirA* mutation. (a and b) Genetic maps of the rhizobactin 1021 synthesis/uptake and putative hemin uptake clusters (a) and a selection of putative energy metabolism gene clusters which are induced in the *rirA* mutant and under iron-limited conditions (b). (c) Gene cluster putatively involved in Fe-S cluster formation which is induced only in the *S. meliloti rirA* mutant. The numbers below the genes indicate the log₂ expression ratios of the genes derived from the microarray-based transcriptome analysis. Genes that were significantly induced in at least one experiment are indicated by solid arrows. The values in parentheses are expression ratios that were below the threshold used in this study.

designated Rm1021-TR2-3, siderophore overproduction was abolished, as indicated by CAS assays (data not shown), providing evidence that the *rirA*-mediated regulation of siderophore synthesis is dependent on the *rhrA* gene. A putative siderophore synthesis gene (SMa2339) which is possibly involved in the formation of rhizobactin 1021 in a hitherto unknown way is located in the immediate vicinity of *rhtA*. Moreover, a number of putative siderophore type ABC transporter genes (SMa1746, SMb21432, and SMc01659) were found among the genes induced under iron-limiting conditions and in the *rirA* mutant. It is of interesting that according to the original annotation SMb21431 codes for the C terminus of a periplasmic binding protein, but resequencing of the corresponding DNA region showed that in the published sequence an error resulting in a frameshift is present. In fact, SMb21431 and SMb21432 constitute a single open reading frame and are referred to as SMb21432 in this report. In addition to putative siderophore type ABC transporter genes, a chromosomal region encoding a putative hemin ABC transporter was also induced by iron limitation and in the *rirA* mutant (Fig. 4a). This putative hemin transporter is encoded by *hmuP*, *hmuS*, *hmuT*, *hmuU*, and *hmuV*, which are homologous to heme uptake genes of *Bradyrhizobium japonicum* (38), *R. leguminosarum* (71), and *Y. pestis* (26). The expression ratios of these genes are shown in Fig. 4a. In addition to these genes, *shmR*, encoding an outer membrane receptor for hemin (3), was also significantly induced in the *rirA* mutant and under both iron-limiting conditions. The deregulation of these genes in the *rirA* mutant is also likely to be a major factor contributing to the observed sensitivity to hemin (Fig. 1c). Interestingly, genes coding for hypothetical proteins in the immediate vicinity of the *hmu* transporter genes (Fig. 4a) were also induced both under iron-limiting conditions and in the *rirA* mutant (SMc01514, SMc01516, SMc01517, and SMc01518). Overall, these findings suggest that the secretion and uptake of siderophores and the induction of heme utilization systems are the main strategy that *S. meliloti* uses to counter iron deficiency and that the repression of these systems is mediated by *rirA*. The only non-

siderophore/heme-type iron transporter gene found to be expressed more highly during iron limitation and in the *rirA* mutant was SMc00784, which encodes the periplasmic binding protein of a ferric type ABC transporter. This protein exhibits 52% identity to FbpA of *Mannheimia* (formerly *Pasteurella*) *hemolytica*, which is involved in iron acquisition during pathogenic host invasion (31, 56). Interestingly, no other components of an ABC transporter were located in the vicinity of SMc00784. None of these putative transporters have been characterized yet, and our results indicate that they may play a major role in the adaptation of *S. meliloti* to low-iron conditions. For *rhbA*, *shmR*, and *hmuS* the results of the microarray experiments were verified by quantitative PCR. The same tendencies were found, although the induction ratios obtained in the quantitative PCR experiments were higher than the values obtained in the microarray experiments (data not shown). This is consistent with other experiments in which the Sm6kOligo microarray was used (32).

Curiously, genes encoding the subunits of a putative ferric-type transporter (*afuA* and *afuC*) were downregulated instead of upregulated during iron-limited growth and in the *rirA* mutant. Recent work of Krol and Becker suggested that these genes might in fact be under the control of the phosphate-dependent regulator PhoB (32), and it is possible that despite high levels of homology to ferric-type transporters this transporter might play a different role in *S. meliloti*.

In addition to iron transporter genes, SMc00402, *exbB*, and *exbD* were also found to be derepressed in the *rirA* mutant and in either iron-limited medium. The deduced gene product of SMc00402 exhibits low levels of homology to IrpA (iron-regulated protein A) of *Synechococcus* sp. strain PCC7942 (48), which was proposed to be involved in iron acquisition, and a similar role for SMc00402 might be proposed for *S. meliloti*. The ExbB and ExbD proteins are generally involved in forming the energy-transducing TonB complex, which energizes the transport of iron substrates by specific receptors across the outer membrane (8). It is therefore likely that the *S. meliloti* *exbB* and *exbD* genes are involved in the transport of ferri-siderophores or heme compounds by the corresponding outer membrane receptors. We found that in the genome of *S. meliloti* only one *tonB* homologue could be detected (SMc01515), which was not differentially expressed in response to iron limitation or by the *rirA* mutation. An individual analysis of the microarray experiments with *S. meliloti* grown in TY medium or in VMM under iron-limiting conditions revealed no other genes with homologies to iron acquisition genes, demonstrating that all iron acquisition genes induced under iron-limiting conditions are also affected by the *rirA* mutation, which is strong evidence that the *S. meliloti* RirA protein is the main regulator of iron uptake.

In addition to iron acquisition genes, other genes involved in energy metabolism, noniron transport, and exopolysaccharide synthesis exhibited enhanced levels of expression during iron limitation and in the *rirA* mutant (Table 2). Altogether, 10 electron transport-associated genes were found to be expressed at an elevated level in the *rirA* mutant and under at least one type of iron-limiting growth conditions (SMc01022, *fixN3*, *fixP3*, *qxtA*, *qxtB*, *cyoA*, *cyoB*, *cyoC*, and *cycG*) (Table 2). The *fix-3* gene cluster encodes a putative cytochrome oxidase and represents another iteration of the previously character-

ized *fix-1* and *fix-2* gene clusters (2). While at least either a functional *fix-1* or *fix-2* gene cluster is known to be essential for establishing a successful symbiosis (49), the *fixN3* and *fixP3* genes obviously have functions other than thsoe of their paralogues and, according to our results, are also regulated differently. Overall, the microarray analyses suggest that iron availability might influence the path of the respiratory chain in *S. meliloti*, which is consistent with the results of similar studies of other bacteria (40, 42, 43, 45, 58).

Three of the *S. meliloti* exopolysaccharide genes (*exoW*, *exoY*, and *exoN*) were induced under all three conditions, and two additional genes (*exoO* and *exoV*) were induced in the *rirA* mutant and during growth in iron-limited TY medium and VMM, respectively. These findings are in agreement with previous reports, which described enhanced production of exopolysaccharides in other bacteria as a result of nutrient stress (68, 72). In addition, *katA* encoding a monofunctional catalase was found to be induced in the *rirA* mutant and in iron-limited VMM. Previously, the *S. meliloti* *katA* gene was found to be inducible by H_2O_2 (25) and to be highly expressed in bacteroids (28). Our results demonstrate that the regulation of this gene is also affected by iron availability and the *rirA* gene. Finally, in addition to the activator gene *rhrA* mentioned above, a number of putative transcription regulator genes (SMa1749, SMc04162, SMc01160, and SMb21464) were differentially expressed depending on the *rirA* mutation and under at least one type of iron-limiting conditions. Hence, it is possible that in some cases *rirA*-mediated iron-dependent regulation might be exerted indirectly via these putative regulators, and it would be interesting to elucidate how these regulators contribute to the *rirA*-mediated regulatory network.

In *R. leguminosarum* iron-responsive regulators were detected, which are potential RirA binding sites (74). We conducted in silico searches in the upstream region of genes induced in the *S. meliloti* *rirA* mutant but were not able to identify any iron-responsive regulator-like sequences.

S. meliloti genes involved in cell motility are repressed under iron-limiting conditions but not in the *rirA* mutant. Altogether, 87 genes were differentially expressed during growth in both iron-limited media but were not affected by the *rirA* mutation (Fig. 3, subset A). No function could be assigned to a large portion of these genes (57% of the induced genes and 21% of the repressed genes). A striking observation was that 30 of the downregulated genes are involved in motility. These genes represent 46% of all predicted motility genes of this bacterium. Twenty-four of these repressed motility genes are located in a cluster which represents the *S. meliloti* flagellar regulon (60).

These genes are known to be regulated in a hierarchical order, with VisN and VisR acting as global activators. In iron-limited VMM the *visN* and *visR* genes were also found to be significantly repressed two- to threefold (see Table S1 in the supplemental material), which probably accounts for the massive reduction of motility genes. This is also likely to be the case during growth in iron-limited TY medium, despite the fact that the *visNR* operon was repressed only ~1.4-fold, which is below the threshold that we used in this study.

Moreover, seven additional genes annotated to encode hypothetical proteins (SMc03005, SMc03013, SMc03017, SMc03023, SMc03057, SMc3071, and SMc3072) located in the

motility cluster and four other genes which are putatively involved in chemotaxis (SMc00765, SMc01469, SMc01104, and Smc00975) but are not located in this cluster were also found to be downregulated during iron limitation. It has been reported that C, N, or phosphate starvation in *S. meliloti* results in a reduction in motility (69). Here we provide evidence that iron limitation also negatively affects the expression of motility genes and that this may be caused by reduced transcription of the master activators of the flagellar regulon.

***S. meliloti* genes involved in the biosynthesis of Fe-S clusters are differentially expressed in the *rirA* mutant but not under iron-limiting conditions.** Altogether, 90 genes involved in a variety of functions were differentially expressed in the *rirA* mutant (Fig. 3, subset C) but were not affected by iron availability. Although we are not able to easily distinguish between direct *rirA*-mediated regulation and secondary effects, as proposed above, in at least some cases reasonable hypotheses can be advanced to explain the observed regulation. For instance, a cluster of genes (SMc00530, SMc00531, SMc00532, SMc00533, SMc00302, and SMc00301), including a putative *nifS* gene, was derepressed in the *S. meliloti rirA* mutant background (Fig. 4 c). The products encoded by genes in this cluster were annotated as either hypothetical proteins or putative ABC transporters, but our renewed annotation showed that the products of SMc00301, SMc00530, SMc00531, SMc00532, and SMc00533 exhibited homology to the *E. coli* SufA, SufB, SufC, SufD, and SufS proteins, respectively, which are involved in assembly of Fe-S clusters (18). In *E. coli* and *Erwinia chrysanthemi* these genes are important for iron acquisition and were found to be induced by oxidative stress and iron starvation (33, 36, 44). Thus, it has been assumed that the *suf* genes are specifically adapted to synthesize Fe-S clusters when iron or sulfur metabolism is disrupted by iron starvation or oxidative stress (41). In both enterobacteria the iron-dependent regulation of the *suf* genes was mediated by Fur. Since we demonstrated that in *S. meliloti* numerous usually *fur*-mediated functions are fulfilled by *rirA*, it is resonable to hypothesize that *rirA* might also be involved in the regulation of the *suf* genes. Another possibility is that the oxidative stress generated in the *rirA* mutant by deregulated iron uptake might indirectly lead to the induction of the *suf* homologues in *S. meliloti*. In a recent report an *suf* cluster in *R. leguminosarum* was found to be induced in an *rirA* mutant, which is in accordance with our results. Interestingly, the induction was found to be highest with high iron concentrations (65), possibly indicating that iron-generated oxidative stress also contributes to the regulation of the *suf* genes in *R. leguminosarum*.

Among the downregulated genes, the most striking groups of genes (17 genes) are involved in protein biosynthesis, including the synthesis of ribosomal proteins and elongation factors (see Table S1 in the supplemental material). This observation is probably a secondary effect due to the reduced growth of the *S. meliloti rirA* mutant.

Conclusions. Iron acquisition is an important aspect of the rhizobial life cycle, and iron limitation severely inhibits the effectiveness of the rhizobium-legume symbiosis (29, 37). The large number of genes differentially regulated in response to iron availability found in this study stresses the importance of this micronutrient for *S. meliloti*. Bioassays with the *S. meliloti rirA* mutant clearly demonstrated the importance of the *rirA*

gene for maintaining intracellular iron concentrations below toxic levels under free-living conditions. This finding was supported by the results of the microarray experiments, which implied that *rirA* has a central role in coordinating the transcriptional response with iron availability. In the case of siderophore synthesis and the uptake cluster, we obtained evidence that the *rirA*-dependent regulation is exerted indirectly via the transcriptional activator gene *rhrA*. Furthermore, the number and variety of regulated genes indicate that regulation mediated by *rirA* is not limited to iron acquisition. While it was not the goal of this work to define the RirA regulon on a molecular level, our analyses identified a number of possible directly RirA-regulated genes that may be used as targets for further studies. Overall, the extent of *rirA*-mediated regulation and the phenotypic analyses of the *S. meliloti rirA* mutant revealed striking parallels to *fur*-mediated regulation. It appears that in *S. meliloti* and likely also in *R. leguminosarum* RirA has the role of a central coordinator of iron-dependent regulation, while the Fur proteins in these rhizobia are involved mainly in the regulation of manganese uptake (12, 15, 47). In this study a large number of genes whose expression was previously not known to be affected by iron, as well as uncharacterized genes with previously unknown functions, were identified. This clearly illustrates the need for further analyses to truly understand the iron metabolism of *S. meliloti*. Our study thus was the first global analysis of iron metabolism and its novel form of regulation by *rirA* in a rhizobial species. The full data sets for genes whose expression is affected by iron availability and the *rirA* mutation constitute a sound basis for targeted mutagenesis experiments.

REFERENCES

1. **Baichoo, N., T. Wang, R. Ye, and J. D. Helmann.** 2002. Global analysis of the *Bacillus subtilis* Fur regulon and the iron starvation stimulon. Mol. Microbiol. **45:**1613–1629.
2. **Barnett, M. J., R. F. Fisher, T. Jones, C. Komp, A. P. Abola, F. Barloy-Hubler, L. Bowser, D. Capela, F. Galibert, J. Gouzy, M. Gurjal, A. Hong, L. Huizar, R. W. Hyman, D. Kahn, M. L. Kahn, S. Kalman, D. H. Keating, C. Palm, M. C. Peck, R. Surzycki, D. H. Wells, K. C. Yeh, R. W. Davis, N. A. Federspiel, and S. R. Long.** 2001. Nucleotide sequence and predicted functions of the entire *Sinorhizobium meliloti* pSymA megaplasmid. Proc. Natl. Acad. Sci. USA **98:**9883–9888.
3. **Battistoni, F., R. Platero, R. Duran, C. Cervenansky, J. Battistoni, A. Arias, and E. Fabiano.** 2002. Identification of an iron-regulated, hemin-binding outer membrane protein in *Sinorhizobium meliloti*. Appl. Environ. Microbiol. **68:**5877–5881.
4. **Beaumont, H. J., S. I. Lens, W. N. Reijnders, H. V. Westerhoff, and R. J. van Spanning.** 2004. Expression of nitrite reductase in *Nitrosomonas europaea* involves NsrR, a novel nitrite-sensitive transcription repressor. Mol. Microbiol. **54:**148–158.
5. **Becker, A., H. Berges, E. Krol, C. Bruand, S. Rüberg, D. Capela, E. Lauber, E. Meilhoc, F. Ampe, F. J. de Bruijn, J. Fourment, A. Francez-Charlot, D. Kahn, H. Küster, C. Liebe, A. Pühler, S. Weidner, and J. Batut.** 2004. Global changes in gene expression in *Sinorhizobium meliloti* 1021 under microoxic and symbiotic conditions. Mol. Plant-Microbe Interact. **17:**292–303.
6. **Beringer, J. E.** 1974. R factor transfer in *Rhizobium leguminosarum*. J. Gen. Microbiol. **84:**188–198.
7. **Boyd, J., M. N. Oza, and J. R. Murphy.** 1990. Molecular cloning and DNA sequence analysis of a diphtheria tox iron-dependent regulatory element (*dtxR*) from *Corynebacterium diphtheriae*. Proc. Natl. Acad. Sci. USA **87:**5968–5972.

8. **Braun, V., K. Gunter, and K. Hantke.** 1991. Transport of iron across the outer membrane. Biol. Met. **4:**14–22.

9. **Capela, D., F. Barloy-Hubler, J. Gouzy, G. Bothe, F. Ampe, J. Batut, P. Boistard, A. Becker, M. Boutry, E. Cadieu, S. Dreano, S. Gloux, T. Godrie, A. Goffeau, D. Kahn, E. Kiss, V. Lelaure, D. Masuy, T. Pohl, D. Portetelle, A. Pühler, B. Purnelle, U. Ramsperger, C. Renard, P. Thebault, M. Vandenbol, S. Weidner, and F. Galibert.** 2001. Analysis of the chromosome sequence of the legume symbiont *Sinorhizobium meliloti* strain 1021. Proc. Natl. Acad. Sci. USA **98:**9877–9882.

10. **Carson, K. C., M. J. Dilworth, and A. R. Glenn.** 1992. Siderophore production and iron transport in *Rhizobium leguminosarum* bv viciae Mnf710. J. Plant Nutr. **15:**2203–2220.

11. **Carson, K. C., S. Holliday, A. R. Glenn, and M. J. Dilworth.** 1992. Siderophore and organic acid production in root nodule bacteria. Arch. Microbiol. **157:**264–271.

12. **Chao, T. C., A. Becker, J. Buhrmester, A. Pühler, and S. Weidner.** 2004. The *Sinorhizobium meliloti fur* gene regulates, with dependence on Mn(II), transcription of the *sitABCD* operon, encoding a metal-type transporter. J. Bacteriol. **186:**3609–3620.

13. **Cuiv, P. O., P. Clarke, D. Lynch, and M. O'Connell.** 2004. Identification of *rhtX* and *fptX*, novel genes encoding proteins that show homology and function in the utilization of the siderophores rhizobactin 1021 by *Sinorhizobium meliloti* and pyochelin by *Pseudomonas aeruginosa*, respectively. J. Bacteriol. **186:**2996–3005.

14. **Delgado, M. J., E. J. Bedmar, and J. A. Downie.** 1998. Genes involved in the formation and assembly of rhizobial cytochromes and their role in symbiotic nitrogen fixation. Adv. Microb. Physiol. **40:**191–231.

15. **Diaz-Mireles, E., M. Wexler, G. Sawers, D. Bellini, J. D. Todd, and A. W. Johnston.** 2004. The Fur-like protein Mur of *Rhizobium leguminosarum* is a Mn^{2+}-responsive transcriptional regulator. Microbiology **150:**1447–1456.

16. **Dondrup, M., A. Goesmann, D. Bartels, J. Kalinowski, L. Krause, B. Linke, O. Rupp, A. Sczyrba, A. Pühler, and F. Meyer.** 2003. EMMA: a platform for consistent storage and efficient analysis of microarray data. J. Biotechnol. **106:**135–146.

17. **Escolar, L., J. Perez-Martin, and V. de Lorenzo.** 1999. Opening the iron box: transcriptional metalloregulation by the Fur protein. J. Bacteriol. **181:**6223–6229.

18. **Flint, D. H.** 1996. *Escherichia coli* contains a protein that is homologous in function and N-terminal sequence to the protein encoded by the *nifS* gene of *Azotobacter vinelandii* and that can participate in the synthesis of the Fe-S cluster of dihydroxy-acid dehydratase. J. Biol. Chem. **271:**16068–16074.

19. **Galibert, F., T. M. Finan, S. R. Long, A. Pühler, P. Abola, F. Ampe, F. Barloy-Hubler, M. J. Barnett, A. Becker, P. Boistard, G. Bothe, M. Boutry, L. Bowser, J. Buhrmester, E. Cadieu, D. Capela, P. Chain, A. Cowie, R. W. Davis, S. Dreano, N. A. Federspiel, R. F. Fisher, S. Gloux, T. Godrie, A. Goffeau, B. Golding, J. Gouzy, M. Gurjal, I. Hernandez-Lucas, A. Hong, L. Huizar, R. W. Hyman, T. Jones, D. Kahn, M. L. Kahn, S. Kalman, D. H. Keating, E. Kiss, C. Komp, V. Lelaure, D. Masuy, C. Palm, M. C. Peck, T. M. Pohl, D. Portetelle, B. Purnelle, U. Ramsperger, R. Surzycki, P. Thebault, M. Vandenbol, F. J. Vorhölter, S. Weidner, D. H. Wells, K. Wong, K. C. Yeh, and J. Batut.** 2001. The composite genome of the legume symbiont *Sinorhizobium meliloti*. Science **293:**668–672.

20. **Grant, S. G., J. Jessee, F. R. Bloom, and D. Hanahan.** 1990. Differential plasmid rescue from transgenic mouse DNAs into *Escherichia coli* methylation-restriction mutants. Proc. Natl. Acad. Sci. USA **87:**4645–4649.

21. **Hamza, I., S. Chauhan, R. Hassett, and M. R. O'Brian.** 1998. The bacterial Irr protein is required for coordination of heme biosynthesis with iron availability. J. Biol. Chem. **273:**21669–21674.

22. **Hantke, K.** 2001. Iron and metal regulation in bacteria. Curr. Opin. Microbiol. **4:**172–177.

23. **Hantke, K.** 1981. Regulation of ferric iron transport in *Escherichia coli* K12: isolation of a constitutive mutant. Mol. Gen. Genet. **182:**288–292.

24. **Hassett, D. J., P. A. Sokol, M. L. Howell, J. F. Ma, H. T. Schweizer, U. Ochsner, and M. L. Vasil.** 1996. Ferric uptake regulator (Fur) mutants of *Pseudomonas aeruginosa* demonstrate defective siderophore-mediated iron uptake, altered aerobic growth, and decreased superoxide dismutase and catalase activities. J. Bacteriol. **178:**3996–4003.

25. **Herouart, D., S. Sigaud, S. Moreau, P. Frendo, D. Touati, and A. Puppo.** 1996. Cloning and characterization of the *katA* gene of *Rhizobium meliloti* encoding a hydrogen peroxide-inducible catalase. J. Bacteriol. **178:**6802–6809.

26. **Hornung, J. M., H. A. Jones, and R. D. Perry.** 1996. The *hmu* locus of *Yersinia pestis* is essential for utilization of free haemin and haem-protein complexes as iron sources. Mol. Microbiol. **20:**725–739.

27. **Horton, R. M.** 1995. PCR-mediated recombination and mutagenesis. SOEing together tailor-made genes. Mol. Biotechnol. **3:**93–99.

28. **Jamet, A., S. Sigaud, G. Van de Sype, A. Puppo, and D. Herouart.** 2003. Expression of the bacterial catalase genes during *Sinorhizobium meliloti*-*Medicago sativa* symbiosis and their crucial role during the infection process. Mol. Plant-Microbe Interact. **16:**217–225.

29. **Johnston, A. W., K. H. Yeoman, and M. Wexler.** 2001. Metals and the

rhizobial-legume symbiosis—uptake, utilization and signalling. Adv. Microb. Physiol. **45:**113–156.

30. **Keon, R. G., R. Fu, and G. Voordouw.** 1997. Deletion of two downstream genes alters expression of the *hmc* operon of *Desulfovibrio vulgaris* subsp. *vulgaris* Hildenborough. Arch. Microbiol. **167:**376–383.

31. **Kirby, S. D., F. A. Lainson, W. Donachie, A. Okabe, M. Tokuda, O. Hatase, and A. B. Schryvers.** 1998. The *Pasteurella haemolytica* 35 kDa iron-regulated protein is an FbpA homologue. Microbiology **144:**3425–3436.

32. **Krol, E., and A. Becker.** 2004. Global transcriptional analysis of the phosphate starvation response in *Sinorhizobium meliloti* strains 1021 and 2011. Mol. Genet. Genomics **272:**1–17.

33. **Lee, J. H., W. S. Yeo, and J. H. Roe.** 2004. Induction of the *sufA* operon encoding Fe-S assembly proteins by superoxide generators and hydrogen peroxide: involvement of OxyR, IHF and an unidentified oxidant-responsive factor. Mol. Microbiol. **51:**1745–1755.

34. **Lynch, D., J. O'Brien, T. Welch, P. Clarke, P. O. Cuiv, J. H. Crosa, and M. O'Connell.** 2001. Genetic organization of the region encoding regulation, biosynthesis, and transport of rhizobactin 1021, a siderophore produced by *Sinorhizobium meliloti*. J. Bacteriol. **183:**2576–2585.

35. **Meade, H. M., S. R. Long, G. B. Ruvkum, S. E. Brown, and F. M. Ausubel.** 1982. Physical and genetic characterization of symbiotic and auxotrophic mutants of *Rhizobium meliloti* induced by transposon Tn5 mutagenesis. J. Bacteriol. **149:**114–122.

36. **Nachin, L., L. Loiseau, D. Expert, and F. Barras.** 2003. SufC: an unorthodox cytoplasmic ABC/ATPase required for [Fe-S] biogenesis under oxidative stress. EMBO J. **22:**427–437.

37. **Nadler, K. D., A. W. Johnston, J. W. Chen, and T. R. John.** 1990. A *Rhizobium leguminosarum* mutant defective in symbiotic iron acquisition. J. Bacteriol. **172:**670–677.

38. **Nienaber, A., H. Hennecke, and H. M. Fischer.** 2001. Discovery of a haem uptake system in the soil bacterium *Bradyrhizobium japonicum*. Mol. Microbiol. **41:**787–800.

39. **Noya, F., A. Arias, and E. Fabiano.** 1997. Heme compounds as iron sources for nonpathogenic *Rhizobium* bacteria. J. Bacteriol. **179:**3076–3078.

40. **Ochsner, U. A., P. J. Wilderman, A. I. Vasil, and M. L. Vasil.** 2002. GeneChip expression analysis of the iron starvation response in *Pseudomonas aeruginosa*: identification of novel pyoverdine biosynthesis genes. Mol. Microbiol. **45:**1277–1287.

41. **Outten, F. W., O. Djaman, and G. Storz.** 2004. A *suf* operon requirement for Fe-S cluster assembly during iron starvation in *Escherichia coli*. Mol. Microbiol. **52:**861–872.

42. **Palma, M., S. Worgall, and L. E. Quadri.** 2003. Transcriptome analysis of the *Pseudomonas aeruginosa* response to iron. Arch. Microbiol. **180:**374–379.

43. **Palyada, K., D. Threadgill, and A. Stintzi.** 2004. Iron acquisition and regulation in *Campylobacter jejuni*. J. Bacteriol. **186:**4714–4729.

44. **Patzer, S. I., and K. Hantke.** 1999. SufS is a NifS-like protein, and SufD is necessary for stability of the [2Fe-2S] FhuF protein in *Escherichia coli*. J. Bacteriol. **181:**3307–3309.

45. **Paustian, M. L., B. J. May, and V. Kapur.** 2001. *Pasteurella multocida* gene expression in response to iron limitation. Infect. Immun. **69:**4109–4115.

46. **Persmark, M., P. Pittman, J. S. Buyer, B. Schwyn, P. R. Gill, and J. B. Neilands.** 1993. Isolation and structure of rhizobactin-1021, a siderophore from the alfalfa symbiont *Rhizobium meliloti* 1021. J. Am. Chem. Soc. **115:**3950–3956.

47. **Platero, R., L. Peixoto, M. R. O'Brian, and E. Fabiano.** 2004. Fur is involved in manganese-dependent regulation of *mntA* (*sitA*) expression in *Sinorhizobium meliloti*. Appl. Environ. Microbiol. **70:**4349–4355.

48. **Reddy, K. J., G. S. Bullerjahn, D. M. Sherman, and L. A. Sherman.** 1988. Cloning, nucleotide sequence, and mutagenesis of a gene (*irpA*) involved in iron-deficient growth of the cyanobacterium *Synechococcus* sp. strain PCC7942. J. Bacteriol. **170:**4466–4476.

49. **Renalier, M. H., J. Batut, J. Ghai, B. Terzaghi, M. Gherardi, M. David, A. M. Garnerone, J. Vasse, G. Truchet, T. Huguet, and P. Boistard.** 1987. A new symbiotic cluster on the pSym megaplasmid of *Rhizobium meliloti* 2011 carries a functional *fix* gene repeat and a *nod* locus. J. Bacteriol. **169:**2231–2238.

50. **Rolfe, B. G., P. M. Gresshoff, and J. Shine.** 1980. Rapid screening for symbiotic mutants of *Rhizobium meliloti* and white clover. Plant Sci. Lett. **19:**277–284.

51. **Rüberg, S., Z. X. Tian, E. Krol, B. Linke, F. Meyer, Y. Wang, A. Pühler, S. Weidner, and A. Becker.** 2003. Construction and validation of a *Sinorhizobium meliloti* whole genome DNA microarray: genome-wide profiling of osmoadaptive gene expression. J. Biotechnol. **106:**255–268.

52. **Sambrook, J., E. F. Fritsch, and T. Maniatis.** 1989. Molecular cloning: a laboratory manual, 2nd ed. Cold Spring Harbor Laboratory, Cold Spring Harbor, N.Y.

53. **Schäfer, A., A. Tauch, W. Jäger, J. Kalinowski, G. Thierbach, and A. Pühler.** 1994. Small mobilizable multi-purpose cloning vectors derived from the *Escherichia coli* plasmids pK18 and pK19: selection of defined deletions in the chromosome of *Corynebacterium glutamicum*. Gene **145:**69–73.

54. **Schwartz, C. J., J. L. Giel, T. Patschkowski, C. Luther, F. J. Ruzicka, H. Beinert, and P. J. Kiley.** 2001. IscR, an Fe-S cluster-containing transcription

factor, represses expression of *Escherichia coli* genes encoding Fe-S cluster assembly proteins. Proc. Natl. Acad. Sci. USA **98:**14895–14900.

55. **Schwyn, B., and J. B. Neilands.** 1987. Universal chemical assay for the detection and determination of siderophores. Anal. Biochem. **160:**47–56.

56. **Shouldice, S. R., D. R. Dougan, P. A. Williams, R. J. Skene, G. Snell, D. Scheibe, S. Kirby, D. J. Hosfield, D. E. McRee, A. B. Schryvers, and L. W. Tari.** 2003. Crystal structure of *Pasteurella haemolytica* ferric ion-binding protein A reveals a novel class of bacterial iron-binding proteins. J. Biol. Chem. **278:**41093–41098.

57. **Simon, R., U. B. Priefer, and A. Pühler.** 1983. A broad host range mobilization system for in vitro genetic engineering: transposon mutagenesis in gram negative bacteria. Bio/Technology **1:**784–791.

58. **Singh, A. K., L. M. McIntyre, and L. A. Sherman.** 2003. Microarray analysis of the genome-wide response to iron deficiency and iron reconstitution in the cyanobacterium *Synechocystis* sp. PCC 6803. Plant Physiol. **132:**1825–1839.

59. **Smith, M. J., J. N. Shoolery, B. Schwyn, I. Holden, and J. B. Neilands.** 1985. Rhizobactin, a structurally novel siderophore from *Rhizobium meliloti*. J. Am. Chem. Soc. **107:**1739–1743.

60. **Sourjik, V., W. Sterr, J. Platzer, I. Bos, M. Haslbeck, and R. Schmitt.** 1998. Mapping of 41 chemotaxis, flagellar and motility genes to a single region of the *Sinorhizobium meliloti* chromosome. Gene **223:**283–290.

61. **Spaink, H. P.** 2000. Root nodulation and infection factors produced by rhizobial bacteria. Annu. Rev. Microbiol. **54:**257–288.

62. **Staggs, T. M., J. D. Fetherston, and R. D. Perry.** 1994. Pleiotropic effects of a *Yersinia pestis fur* mutation. J. Bacteriol. **176:**7614–7624.

63. **Stojiljkovic, I., B. D. Evavold, and V. Kumar.** 2001. Antimicrobial properties of porphyrins. Expert Opin. Investig. Drugs **10:**309–320.

64. **Todd, J. D., M. Wexler, G. Sawers, K. H. Yeoman, P. S. Poole, and A. W. Johnston.** 2002. RirA, an iron-responsive regulator in the symbiotic bacterium *Rhizobium leguminosarum*. Microbiology **148:**4059–4071.

65. **Todd, J. D., G. Sawers, K. H., and A. W. Johnston.** 2005. Proteomic analysis reveals the wide-ranging effects of the novel, iron-responsive regulator RirA in *Rhizobium leguminosarum* bv. *viciae*. Mol. Genet. Genomics **273:**197–206.

66. **Touati, D., M. Jacques, B. Tardat, L. Bouchard, and S. Despied.** 1995. Lethal oxidative damage and mutagenesis are generated by iron in Δ*fur* mutants of *Escherichia coli*: protective role of superoxide dismutase. J. Bacteriol. **177:**2305–2314.

67. **Vincent, J. M.** 1970. A manual for the practical study of root nodule bacteria. IBP handbook no. 15. Oxford University Press, Oxford, United Kingdom.

68. **Wai, S. N., Y. Mizunoe, A. Takade, S. I. Kawabata, and S. I. Yoshida.** 1998. *Vibrio cholerae* O1 strain TSI-4 produces the exopolysaccharide materials that determine colony morphology, stress resistance, and biofilm formation. Appl. Environ. Microbiol. **64:**3648–3655.

69. **Wei, X., and W. D. Bauer.** 1998. Starvation-induced changes in motility, chemotaxis, and flagellation of *Rhizobium meliloti*. Appl. Environ. Microbiol. **64:**1708–1714.

70. **Wexler, M., J. D. Todd, O. Kolade, D. Bellini, A. M. Hemmings, G. Sawers, and A. W. Johnston.** 2003. Fur is not the global regulator of iron uptake genes in *Rhizobium leguminosarum*. Microbiology **149:**1357–1365.

71. **Wexler, M., K. H. Yeoman, J. B. Stevens, N. G. de Luca, G. Sawers, and A. W. Johnston.** 2001. The *Rhizobium leguminosarum tonB* gene is required for the uptake of siderophore and haem as sources of iron. Mol. Microbiol. **41:**801–816.

72. **Wrangstadh, M., P. L. Conway, and S. Kjelleberg.** 1986. The production and release of an extracellular polysaccharide during starvation of a marine *Pseudomonas* sp. and the effect thereof on adhesion. Arch. Microbiol. **145:**220–227.

73. **Yang, Y. H., S. Dudoit, P. Luu, D. M. Lin, V. Peng, J. Ngai, and T. P. Speed.** 2002. Normalization for cDNA microarray data: a robust composite method addressing single and multiple slide systematic variation. Nucleic Acids Res. **30:**e15.

74. **Yeoman, K. H., A. R. Curson, J. D. Todd, G. Sawers, and A. W. Johnston.** 2004. Evidence that the *Rhizobium* regulatory protein RirA binds to cis-acting iron-responsive operators (IROs) at promoters of some Fe-regulated genes. Microbiology **150:**4065–4074.